



OPEN Polishing dental ceramics using shear-thickening slurry

Zhenfeng Zhou^{1,2,3}, Lijun Zhu^{1,2}, Jiayu Wang¹ & Xiaoxing Dong^{1,2,3}✉

Nowadays, there is a great demand for Zirconia dental ceramics, while the existing low-cost automated polishing methods are quite limited. We propose a novel polishing methodology employing the shear-thickening slurry (STF) comprising starch and SiC abrasive particles. This polishing method enhances viscosity under applied pressure, offering an approach to address the identified challenge. A series of polishing experiments and an in vitro study are conducted to assess the effectiveness of this method compared to manual polishing. The feasibility of the proposed method for polishing dental veneer and crown ceramics is investigated as well. With 2000# SiC-STF slurry, 300 r/min fixture and 120 r/min workpiece, the minimum surface roughness Ra of polished surface can reach 9.5 nm after 30 min. Furthermore, both the novel and manual polishing methods result in samples with comparable flexural strength. Importantly, the innovative use of STF exclusively employs mechanical friction for material removal, circumventing potential chemical erosion. This work can bring a low-cost, efficient, and non-toxic automated polishing method for dental ceramics.

Keywords Shear thickening fluid, Rheology, Dental ceramics, Mechanical properties, Ultra-precision machining

With advancements in dental technology, dental ceramics are valued for their natural aesthetics, biocompatibility, and durability^{1–3}. However, challenges like friction, wear, and biological corrosion^{4–6} can diminish their longevity and glossiness. Polishing dental ceramics is essential for enhancing aesthetics and quality⁷, and for reducing plaque buildup and dental issues, making it vital for ceramic restorations.

Research on dental ceramic polishing techniques aims to improve surface quality, enhance aesthetic appeal, and prolong longevity⁸. Challenges remain in selecting suitable polishing methods, establishing optimal protocols, and defining evaluation criteria^{9,10}. Addressing these challenges is critical for advancing the field. In the present situation, dental ceramics are polished in crown factories by technicians or dentists in clinics or hospitals using diverse polishing tool kits^{11,12}. Ji et al.¹³ compared the grinding and polishing efficiency of self-glazed zirconia and Zenostar zirconia using the same fine rubber diamond polisher, revealing higher efficiency with self-glazed zirconia. This underscored how variations in the finishing quality of manually polished dental ceramics stem from differences not only in ceramic materials but also in dentists' proficiency. The most challenging aspect lies in the time-consuming process of tooth crown fabrication, encompassing rough and fine polishing stages with various materials. Additionally, manual polishing can generate numerous microscale or nanoscale particles, posing an inhalation risk to dentists. Due to its labor-intensive nature, the dental ceramic processing trend leans towards automated polishing.

Researchers have explored automated polishing of dental ceramics using various polishing kits. Yuki et al.¹⁴ developed a dry polishing machine using a sodium alginate-bonded silicon carbide wheel for dental composite material. They achieved a significant reduction in surface roughness from 0.6 μm to 0.06 μm after polishing², although it remained at a sub-micrometer level. Mokhtar et al.¹⁵ explored different surface treatments' impact on bond strength in lithium silicate dental ceramics. They found that acid etching finishing outperformed sandblasting polishing while cautioning against laser treatment due to its potential to alter surface properties. Laser irradiation can affect morphology, roughness, and wettability, especially in materials like zirconium oxide¹⁶. Although laser polishing holds potential for ceramic modification, its efficacy varied based on the ceramic type and clinical context, considering factors like cost, time, and material integrity in dental practice. Loh et al.¹⁷ demonstrated that magnetic field-assisted batch polishing was highly effective and efficient for mass polishing dental zirconia crowns, yielding minimal surface roughness and flexural strength comparable to manual methods. Due to the complexity of magnetic field equipment and the requirement for high-quality magnetic abrasive, batch polishing dental ceramics face cost challenges, warranting the exploration of more efficient and cost-effective alternatives. Mainstream methods such as bonnet polishing¹⁸, fluid jet polishing¹⁹,

¹Provincial Key Laboratory of Multimodal Perceiving and Intelligent Systems, Jiaxing University, Jiaxing 314001, China. ²College of Information Science and Engineering, Jiaxing University, Jiaxing 314001, China. ³G60 STI Valley Industry & Innovation Institute, Jiaxing 314001, China. ✉email: dongxiaoxing@zjxu.edu.cn

and magnetorheological finishing²⁰ were costly and impractical for polishing dental ceramics. As a result, manual polishing remains the go-to approach. Meanwhile, material fields are actively seeking eco-friendly and easy-to-produce mediums for efficient processing. Recently, Li et al.^{21,22} introduced a shear-thickening polishing method using a non-Newtonian power-law fluid slurry with a multi-hydroxyl polymer to enhance surface quality. This technique leverages viscosity increase under high shear stress, allowing for STF application without extra magnetic or electric field equipment in the polishing area. As reported by Gürgen et al.²³, STP, employing nano-sized fumed silica and abrasive particles, had enhanced surface finishes for steel bars. Its versatility was evident in applications such as cemented carbide inserts²⁴, turbine blades²⁵, and gears²⁶. Considering its potential cost-effectiveness, the use of STF may enable automated polishing of dental ceramics. STF polishing shares the same drag-and-rotate mechanics as conventional abrasive finishing^{27,28}, it simply swaps scarce minerals for cheap, biodegradable starch, cutting media costs to a fraction.

In this study, the rheological properties of shear-thickening slurries were measured by incorporating silicon carbide (SiC) abrasives into a low-cost starch-based fluid. These slurries were utilized for polishing zirconia ceramics, and their impact on dental ceramic processing was assessed through Energy Dispersive Spectrometer (EDS) analysis and bending experiments. Finally, the effect of polishing was evaluated by analyzing the surface roughness of dental veneers and crown ceramics before and after polishing in dental technology. Unlike manual or drag/rotational abrasive finishing, this starch-based STF process taps a cheap, abundant medium, runs fully automated, and polishes parts in one batch.

Materials and methods

Polishing methodology

Figure 1 shows the working principle of the polishing method using STF. As illustrated in Fig. 1(a), shear-thickening slurries prevent a bowling ball from immediately sinking into the liquid's surface by altering its viscosity based on shear rate changes. At low rates, colloidal particles disperse and shear thin, but upon impact, the shear rate rises, causing particles to cluster and viscosity to surge, as shown in Fig. 1(b). Emulating the full-aperture magnetic fluid method, shear-thickening slurries are introduced into the cylinder processing equipment, as detailed in Fig. 1(c). During motion between the workpiece and slurries, the high-viscosity shear is generated, allowing for effective dental ceramic polishing with the hard SiC abrasive particles or other polishing abrasive particles. This approach, akin to magnetic fluid processing but without extra equipment, offers a more cost-effective solution.

Materials and sample preparation

The STF, consisting mainly of cassava starch and SiC abrasive as the dispersed phase, with deionized water as the continuous phase, was purchased from Qingzhou Beilian Starch Co., Hangzhou Huatian Water Treatment Equipment Co., and Dongguan Baite Abrasive Co., respectively. Additionally, dental ceramic materials,

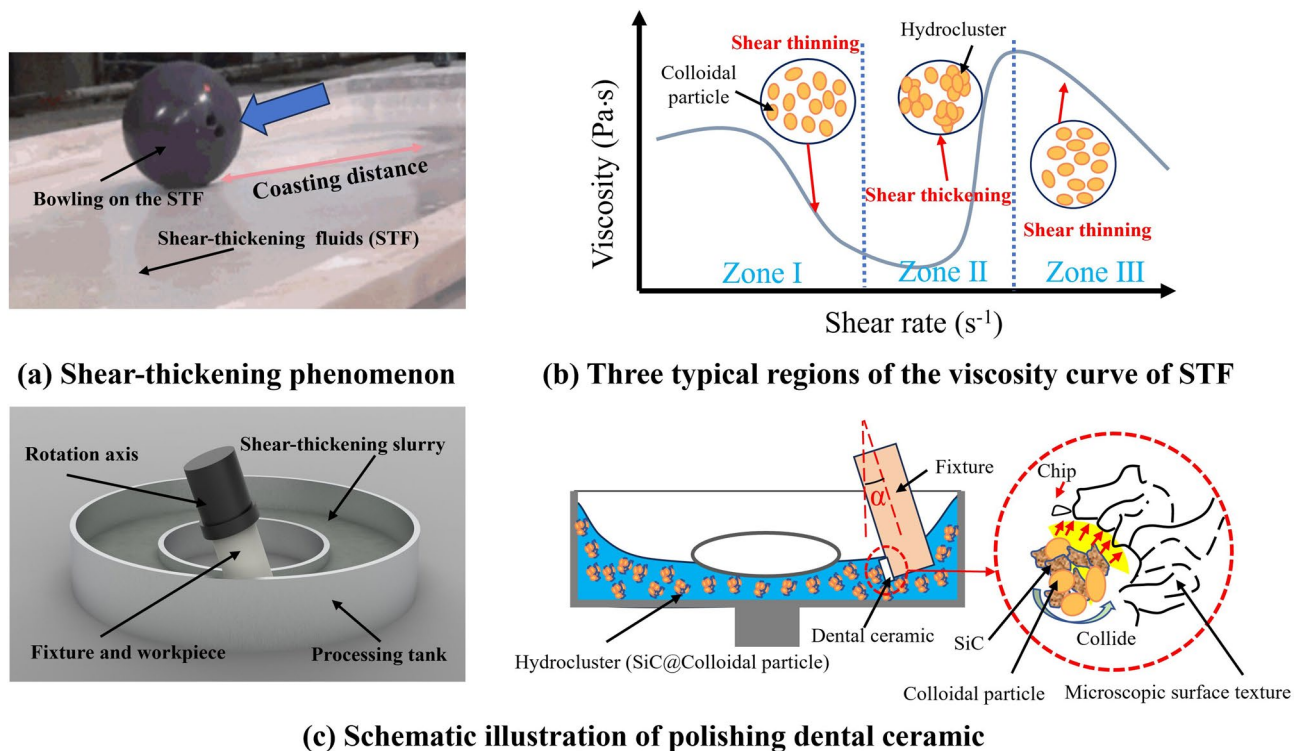


Fig. 1. The working principle of the polishing method using STF.

Groups	Conditions	Parameters(by weight)
1	Shear-thickening fluid	Distilled water: Starch = 45:55
2	STF added 500# SiC abrasives	Distilled water: Starch: SiC = 45:50:5
3	STF added 1000# SiC abrasives	Distilled water: Starch: SiC = 45:50:5
4	STF added 2000# SiC abrasives	Distilled water: Starch: SiC = 45:50:5
5		Distilled water: Starch: SiC = 40:50:10

Table 1. Detailed experimental conditions of the STF.

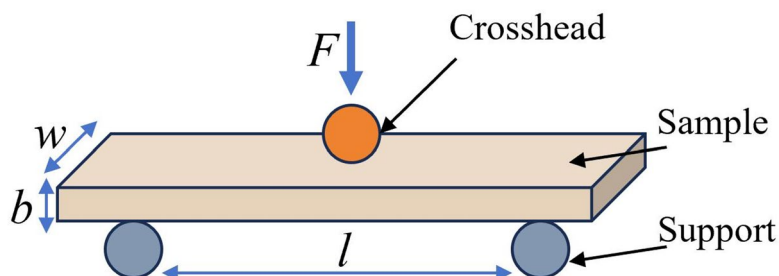


Fig. 2. Schematic diagram of the three-point bending test.

including millable dental zirconia blocks, tubes, dental veneers, and crown ceramics samples, were obtained from Dongguan Zhixunda Medical Equipment Co., Ltd.

The exact compositions of the STF were detailed in Table 1. After thorough stirring and 2-hour equilibration at 25 °C, the STF was ready. Before processing experiments, gave it a 30-minute re-stir and a dynamic 15-minute ultrasonic dispersion to break down aggregates and ensure homogeneity. The zirconia blocks were meticulously sectioned into dimensions of 14.0 mm in length, 5 mm in width, and 2.5 mm in thickness. Similarly, the zirconia tubes were crafted into a hollow cylinder with 1 mm in wall thickness, 8 mm in diameter, and 10 mm in length, intended for the precise polishing of a small sample in the experimental setup. To enhance precision and minimize error, the zirconia ceramic surface was hand-polished for 10 min with 200# SiC sandpaper, yielding an initial roughness between Ra 150 nm and Ra 250 nm.

Material characterization and mechanical tests

The surface morphology of the materials was observed using the NovaNano SEM 450, a high-resolution scanning electron microscope from FEI Company. To address their non-conductivity, all specimens were treated with gold spray before characterization.

The microscopic properties of the shear-thickening slurries were analyzed using KEYENCE's VHX 600 ultra-depth-of-field 3D microscope. This versatile instrument offers a magnification range from 500X to 5000X.

Rheological tests were conducted using an MCR 301 Anton Paar stress-controlled rheometer equipped with a 40 mm diameter parallel plate apparatus. The experiments maintained a constant 0.5 mm gap between the plates while varying the shear rate from 0 to 700 s⁻¹, all at a fixed temperature of 25 °C.

The Mitotoyo SJ410 profiler measured zirconia surface roughness, while the advanced WYKO NT9100 equipment characterized the morphology and roughness of complex ceramic tooth pieces and crowns, surpassing the profiler's limitations. This dual approach provided a comprehensive assessment of polishing effectiveness.

The mass difference before and after processing by STF was obtained by weighing method using XP105 precise analytical balance, and the material removal rate of polishing (MRR) was calculated by Eq. (1):

$$MRR = \frac{\Delta m}{\rho ST} \quad (1)$$

where Δm is the mass difference before and after processing, ρ is the density of zirconia ceramics, S is the polishing area and T is the polishing time.

To examine the influence of surface finishing on the flexural strength of each sample, flexural strength tests were conducted following the ISO 6872 standard for dental zirconia, utilizing a universal testing machine (ElectroPuls E3000, Instron, Norwood, USA). The schematic diagram of the three-point bending test, illustrated in Fig. 2, guided the experimental setup. The distance between the two roller bar supports was maintained at 12 mm. Applying a breaking load (N) with a crosshead featuring a feed rate of 1 mm/min, the recorded data allowed the determination of flexural strength using Eq. (2):

$$\sigma = \frac{3Fl}{2wb^2} \quad (2)$$

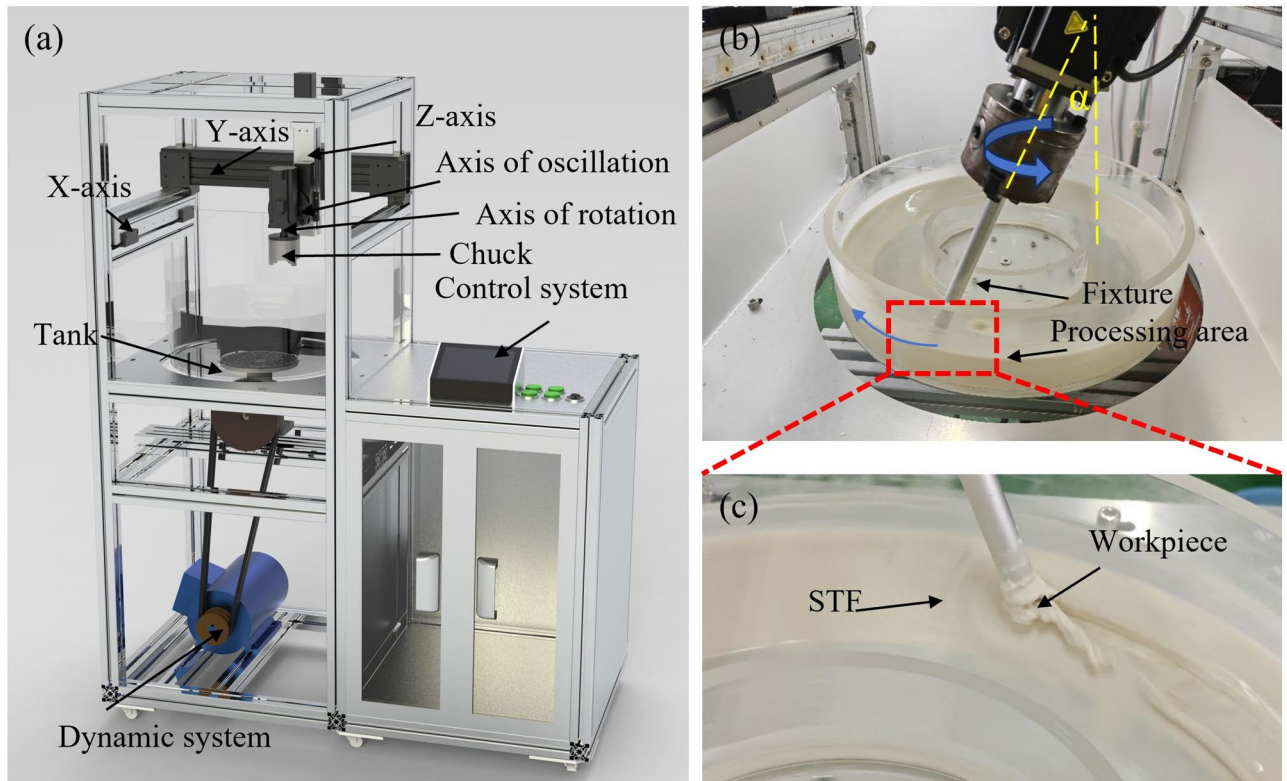


Fig. 3. Shear-thickening polishing system and equipment.

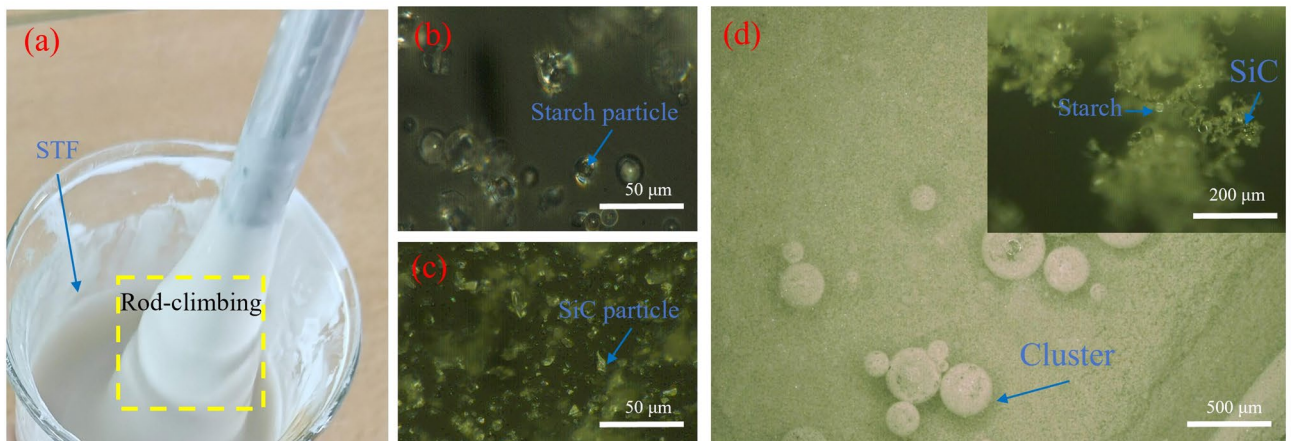


Fig. 4. Macroscopic and microscopic characteristics of shear-thickened slurry.

where F is the breaking load, l is the distance between supports, w and b are the width and thickness of each sample.

Polishing experiment

Figure 3 illustrated our innovative system and equipment designed for polishing based on the shear-thickening principle. A motor-driven turntable supported a cylinder filled with shear-thickening slurries. The zirconia ceramic sample, placed on a fixture, experienced an impact angle of approximately 30° . The logic controller within the control system adjusted the experimental speed instructions.

Results and discussion

Material characterization of shear-thickening slurries

Figure 4 displayed the macroscopic and microscopic characteristics of shear-thickening slurries following the polishing of mixed SiC abrasives. Figure 4(a) illustrated the phenomenon of rod-climbing observed in shear-

thickening slurries. As the slurries ascend the vertical surface at an accelerating rate, its viscosity undergoes an increase. Consequently, the slurries adhered to the rod, giving the impression of the rod elevating the beaker through the slurries. Figure 4(d) depicted the cluster formation of starch particles under high shear, surrounded by sharp-edged SiC abrasives. During processing, these SiC edges impacted the dental ceramic surface, facilitating polishing and finishing.

Figure 5 depicted how the concentration and particle size of added SiC abrasives affected the rheological properties of shear-thickened slurries. Even with only starch particles added, the mixture showed a stable relationship between viscosity and shear rate, displaying both shear-thickening and shear-thinning behaviors. Notably, certain trends stood out as crucial at key points in the results. As the proportion of SiC abrasives in the shear-thickening slurries increased, so did the initial viscosity. This rise could be explained by the increased concentration of solid particles, strengthening particle adhesion. While viscosity typically increased with denser suspensions, the maximum viscosity experienced a geometric rise with every 5% increase in SiC abrasives. For instance, the maximum viscosity started at 537 Pa·s without SiC abrasives addition, but with just a 5% increase, it jumped to ~1075 Pa·s. Consequently, the shear force also increased. Figure 5(b) illustrated the impact of particle size on the initial viscosity of shear-thickening slurries. The rheological curve revealed that initial viscosity increases with larger additive particle sizes. Notably, smaller particles proved more effective in elevating initial viscosity due to their greater dispersion and ease in forming hydrogen bonds. However, it was worth noting that while the maximum viscosity remains unchanged, indicating the total hydrogen bond is linked to substance quantity, particle size generally does not affect this outcome.

Surface roughness and polishing efficiency

Figure 6(a) presented a clear depiction of the efficacy of polishing in enhancing surface roughness within the processing condition of group 4. It also provided a detailed analysis of specific surface roughness values and their respective trends before and after polishing. Following a 40-minute polishing regimen utilizing shear-thickening slurries, the surface roughness R_a of hard zirconia ceramic notably decreased from ~200 nm to ~14 nm. This experimental result underscores the ability of shear-thickening slurries to enhance the surface finish of zirconia ceramics. Subsequently, SEM and EDS analyses of zirconia ceramics were conducted before and after polishing. SEM observation revealed that the SiC abrasive particles effectively remove deep scratches, crucial for reducing roughness. EDS analysis before and after polishing confirmed no contamination of new elements, indicating the shear-thickening slurry's purely mechanical action on the ceramic surface without chemical involvement. The paramount concern for the non-toxicity of medical ceramics implanted within the human body imposes constraints on the utilization of chemical polishing methods for surface refinement. Leveraging the inherent rheological properties of natural starch alongside significant polishing SiC particles presented a viable alternative that circumvents chemical erosion. Moreover, EDS analysis revealed a diminishment in the strength of the Zr element, potentially influencing the mechanical properties of dental ceramics. Consequently, subsequent bending mechanical measurements of dental ceramics were imperative to ascertain any consequential impacts on sub-ceramic quality.

Figure 7(a1) illustrated the dynamic evolution of surface roughness under varying rotation speeds. Each curve corresponded to specific rotation speeds: 40, 80, and 120 r/min. Initially, the measured roughness R_a maintained a consistent value of ~200 nm. However, over time, the differential impact of rotation speeds on surface roughness emerged. Notably, higher rotation speeds exhibited a more pronounced reduction in surface roughness within the initial 10-minute period, attributed to the intensified collision frequency of SiC abrasive particles with the surface. Subsequently, after 40 min of processing, surface roughness R_a stabilized within the

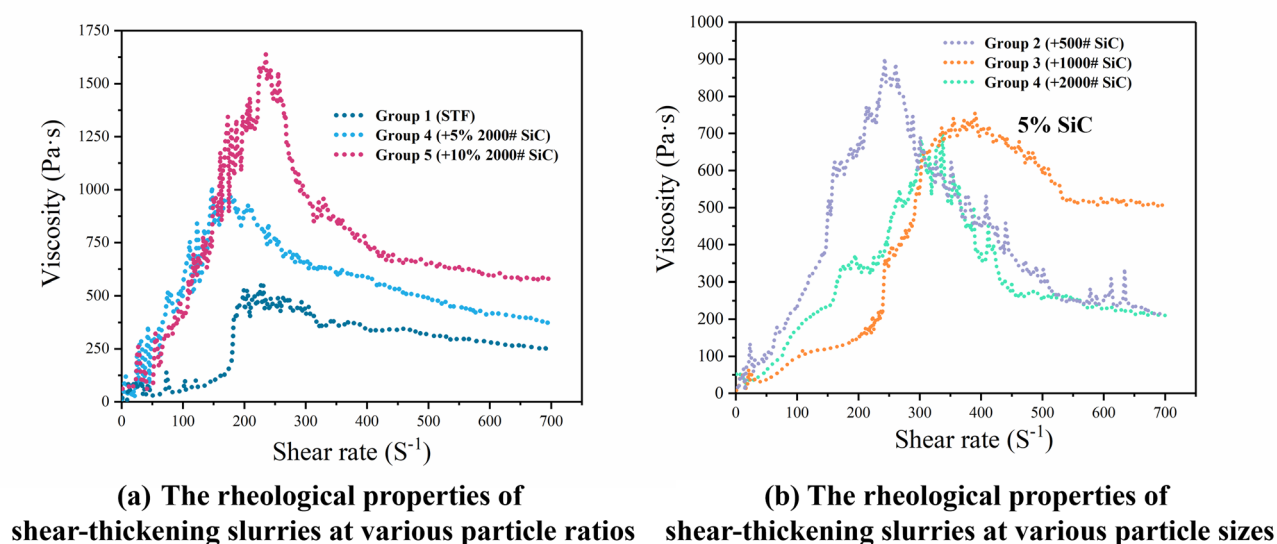


Fig. 5. Rheological properties of shear-thickening slurries.

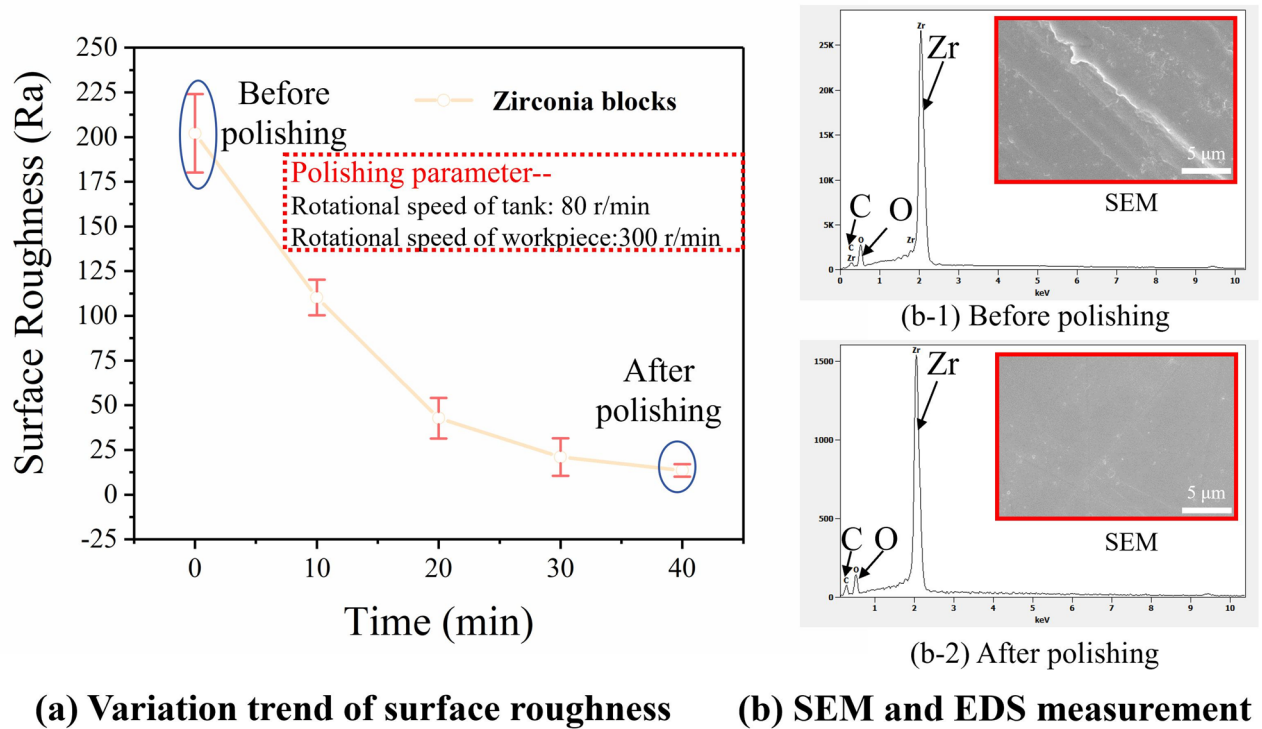


Fig. 6. Polishing results of zirconia ceramic blocks.

range of 10–30 nm. Figure 7(b1) elucidated the variation in surface roughness during polishing processing with differing SiC particle sizes. It is evident that larger particles induce a more rapid decline in surface roughness. Conversely, processing with smaller particles yielded a stable final surface roughness at a higher value. Comparing Fig. 7(a1) and Fig. 7(b1), it is implied that the ultimate roughness stabilization is intricately linked to the cutting edge characteristics of the abrasive particle, whereby smaller edges result in diminished roughness. Upon comparison of the processing efficiency illustrated in Fig. 7(a2) and Fig. 7(b2), it become apparent that higher processing speeds and larger particle sizes led to an increment in the material removal rate (MRR). This observation conformed to the principles outlined in the Preston equation, a widely utilized framework for describing polishing processes. The Preston equation ($KPV = MRR$), where K denotes an empirical coefficient, while P and V signify the contact pressure and processing speed, respectively. Consequently, with the escalation of processing groove speed, the velocity of slurry impact on the workpiece proportionately increased. Furthermore, the SiC particle size, manifested in the rheological characteristics depicted in Fig. 6, induced variations in microscopic contact friction, thereby indirectly influencing the ultimate processing efficiency.

Flexural strength

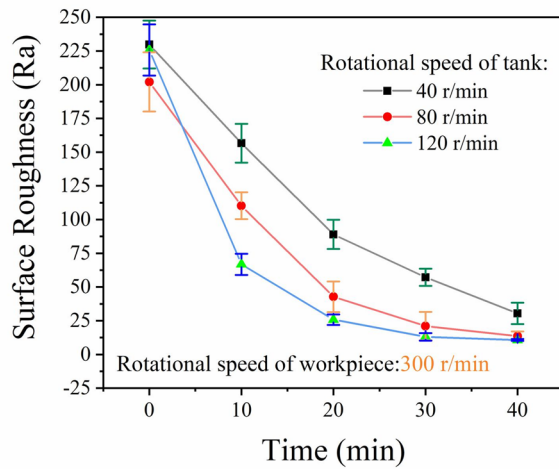
The flexural strength tests were conducted on polishing zirconia blocks, with an additional group of manually lapped samples for comparison, to evaluate the effect of shear-thickening polishing on dental ceramic strength. The zirconia blocks used for testing underwent 3 experiments for each set of the parameters. The results were depicted in Fig. 8. When employing automatic polishing with STF, polished groups exhibited an average flexural strength of 816.2 MPa, while manual lapping yielded a comparable result of 835.7 MPa. Intriguingly, the experimental results indicate no significant difference in flexural strength between machine and manual polishing methods. Furthermore, machine polishing enables rapid and precise polishing of multiple dental zirconia plates. Impressively, the surface roughness Ra of polished samples can reach ~ 15 nm.

Surface topography of zirconia ceramic samples

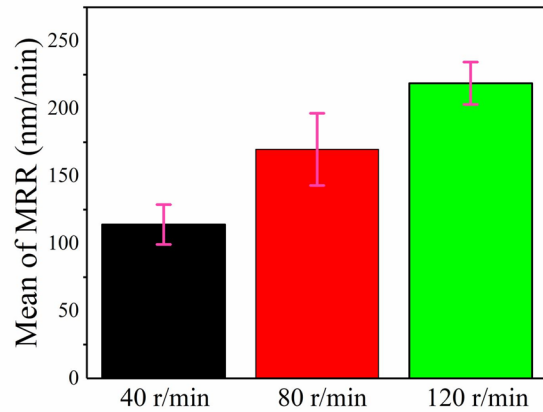
Figure 9 illustrated snapshots and microscopic profiles of zirconia ceramic blocks before and after shear-thickening polishing. As shown in Fig. 9(b), the ultra-depth-of-field 3D microscope revealed the initially roughness surface of zirconia ceramics, marked by numerous processing flaws. After a 40-minute polishing, most flaws were eliminated, reducing surface roughness Ra from 185.3 nm to 15.3 nm, achieving the mirror effect on the sample (see Fig. 9-a).

Ceramic blocks are flat, while dental veneer and crown ceramics are curved. To evaluate polishing effectiveness using STF on surfaces, a 40-minute polishing of the zirconia ceramic tube was conducted, and the results were displayed in Fig. 10.

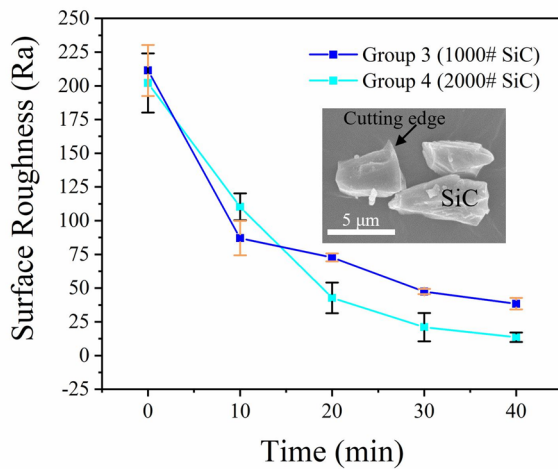
Due to the amorphous nature of the STF, it can entirely envelop the surface of the ceramic tube, forming a “flexible abrasive tool” for polishing. The surface roughness Ra decreased from 218.4 nm before polishing to



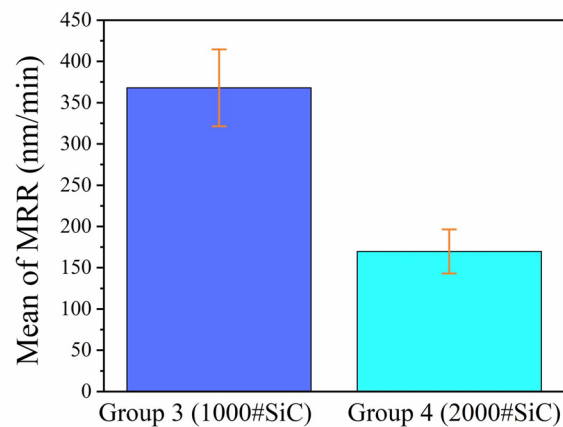
(a-1) Variation trend of surface roughness at different rotational speeds



(a-2) Material removal rate at different rotational speeds



(b-1) Variation trend of surface roughness at different SiC abrasive sizes



(b-2) Material removal rate at different SiC abrasive sizes

Fig. 7. Polishing results of roughness variation and material removal rate of zirconia ceramic blocks under different conditions.

7.8 nm after polishing in processing condition of group 2. Despite the overall improvement in surface roughness, some residual polishing marks and pits remained on the workpiece due to the limitations of the process. Conversely, in ceramic tube polishing, the primary action involved removing SiC abrasive edge burrs through impact, while also leaving behind polished pit marks.

Polishing performance on dental veneer and crown ceramic

To further explore the technical feasibility of shear-thickening on polishing dental veneer, a case study was conducted as shown in Fig. 11. In this experiment, the dental veneer was affixed to the fixture. The fixture rotated at a speed of 300 r/min, while the cylinder processing equipment rotated at 120 r/min. As shown in Fig. 11, it can be found that the improvement of the surface finish is significant. Random measurement locations on the surface, highlighted with blue circles, were compared surface roughness before and after using STF. Before polishing, the surface roughness Ra exceeded 80 nm. After polishing, a significant decrease occurred, with the initial 131.7 nm dropping to 9.5 nm at measurement position 1. Similarly, at measurement position 2, the surface roughness Ra notably decreased, reaching 12.8 nm after polishing.

Figure 12 demonstrated the surface morphology evolution before and after employing STF. Initially covered with profound scratches, the surface undergone significant refinement after a 30-minute application of STF, resulting in a notably smoother texture. This highlights the efficacy of incorporating SiC particles into a shear-

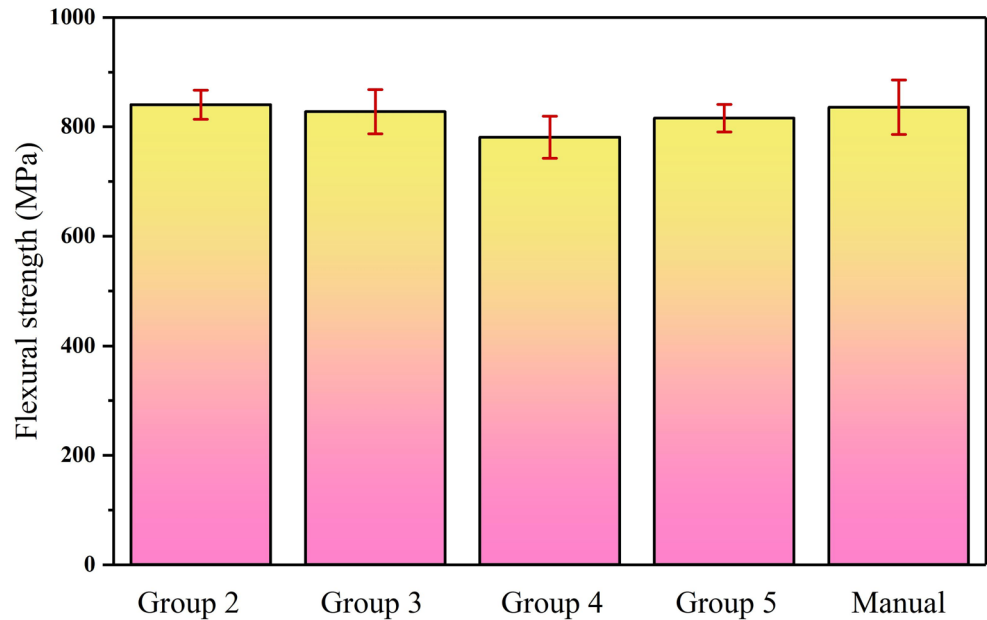


Fig. 8. Flexural strength of different groups after polishing.

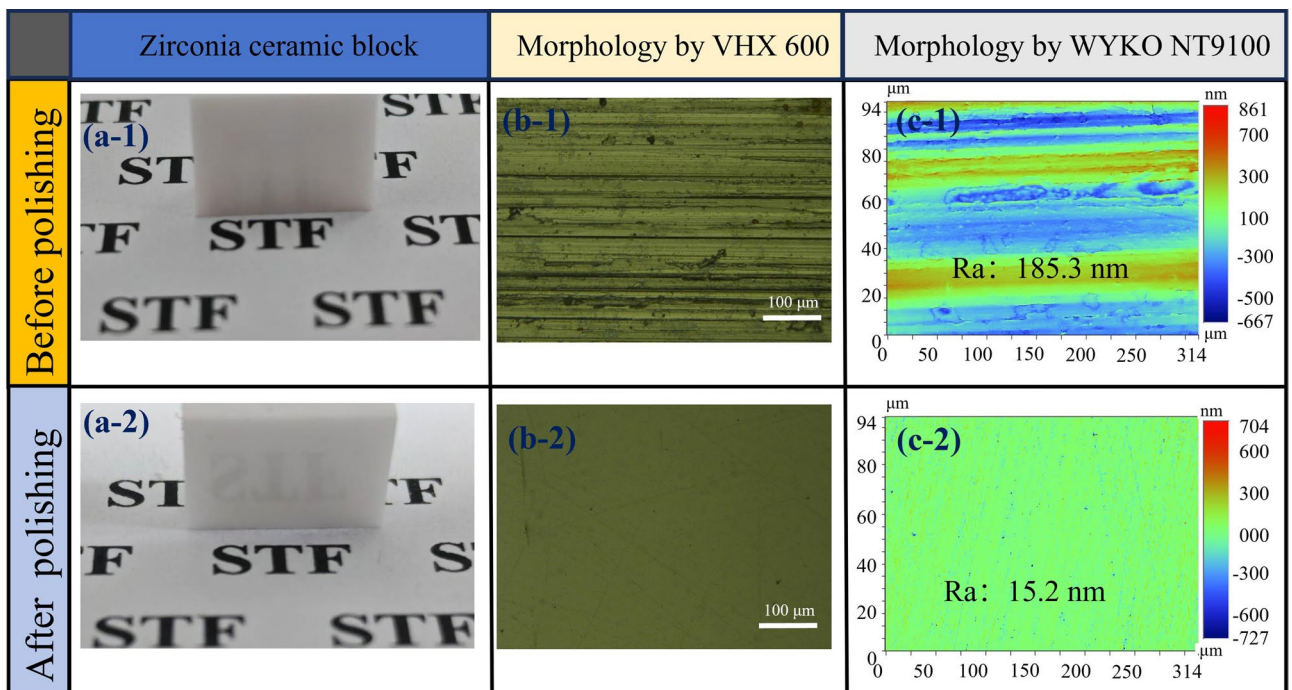


Fig. 9. Surface morphology of zirconia ceramic blocks before and after polishing.

thickening solution comprising natural starch, presenting a promising avenue for enhancing the surface finish of dental ceramic samples, notably dental veneers.

In the realm of dental ceramic polishing, despite the beneficial application of STF, a significant challenge persists: achieving consistent surface roughness across the dental crown, notably within its uppermost groove. Despite a reduction in surface roughness Ra from 248.6 nm to 63.8 nm after a 30-minute polishing period, this discrepancy remained pronounced compared to the lateral surfaces of the dental crown, which experienced a decline from 277.3 nm to 16.2 nm during the same period, as shown in Fig. 13. The accumulation of STF within the crown's apex groove appears to be the root cause, hindering the uniform effectiveness of SiC abrasive particles and impeding surface refinement. Addressing this issue requires efforts to mitigate slurry accumulation, ensuring

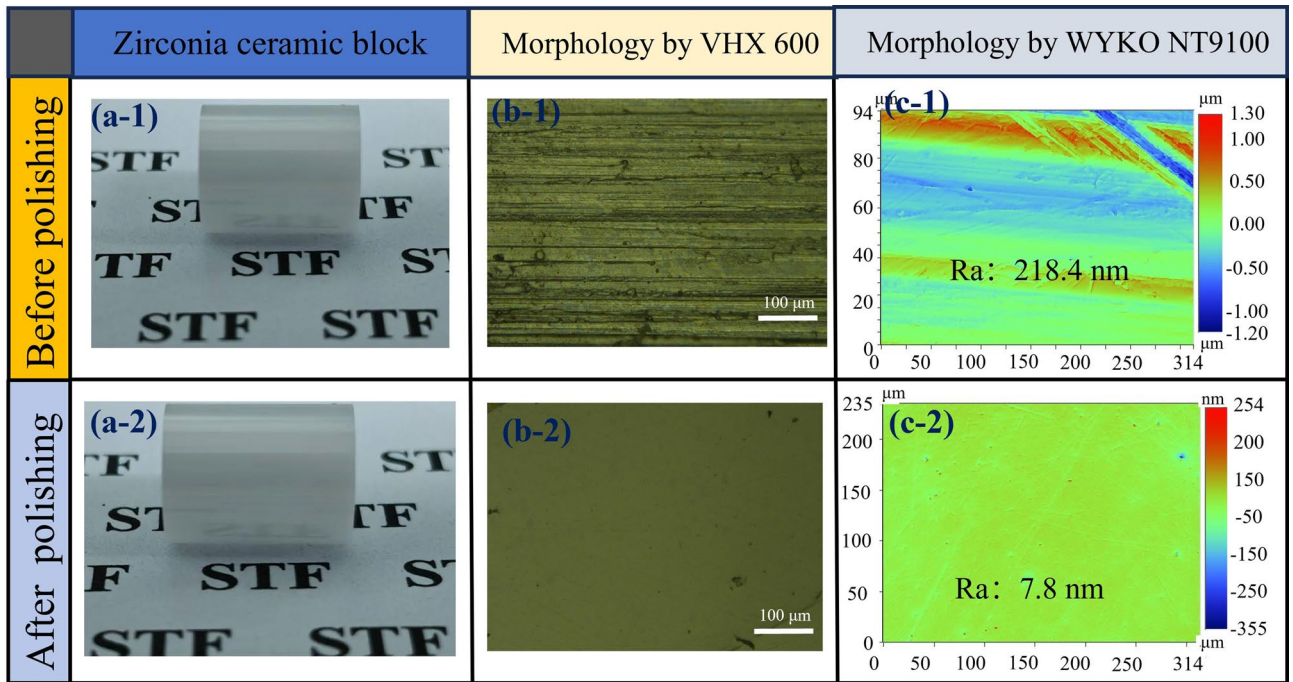


Fig. 10. Surface morphology of zirconia ceramic tube before and after polishing.

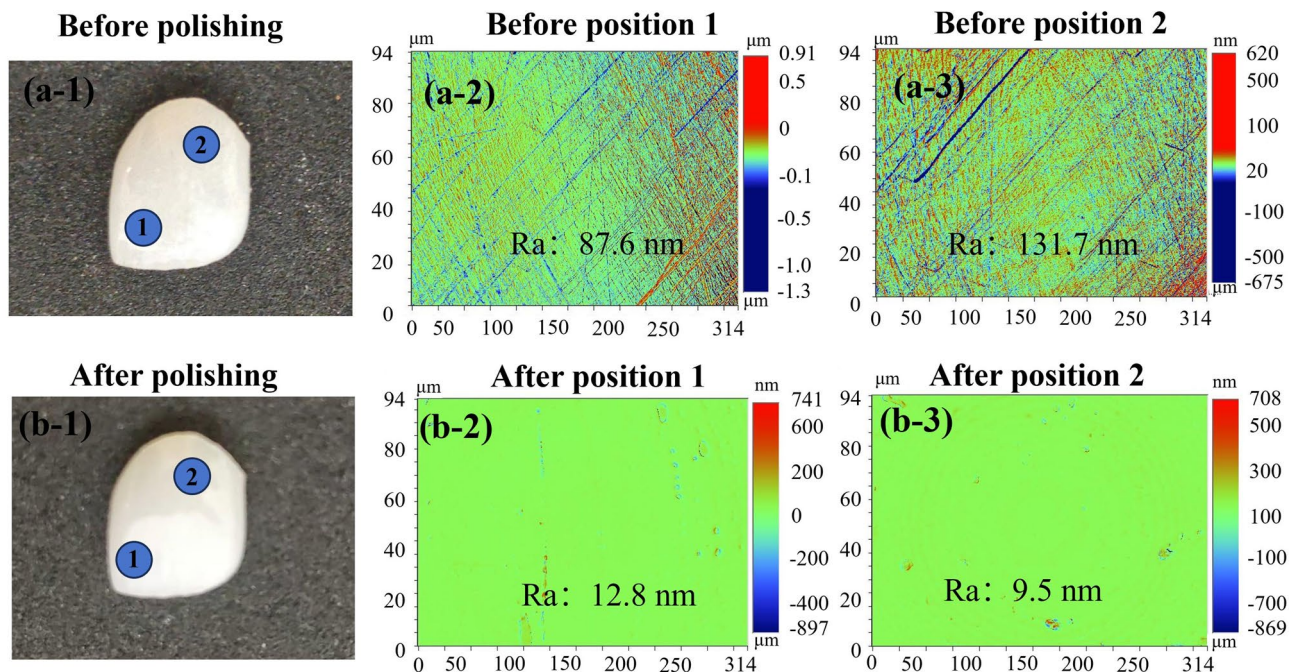


Fig. 11. Polishing performance on the dental veneer using STF.

the uniform distribution of abrasive forces across the entire crown surface. Additionally, the comprehensive exploration of this novel process is imperative to offer valuable insights for practical polishing applications.

Conclusions

This study presents a novel automated approach for polishing dental ceramics using starch-based shear-thickening fluids (STF), demonstrating its advantages over conventional manual grinding through systematic experimental investigations and in vitro assessments. The key findings are as follows: First, STF polishing effectively reduces the surface roughness of zirconia from approximately 200 nm to 9.5 nm within 30 min,

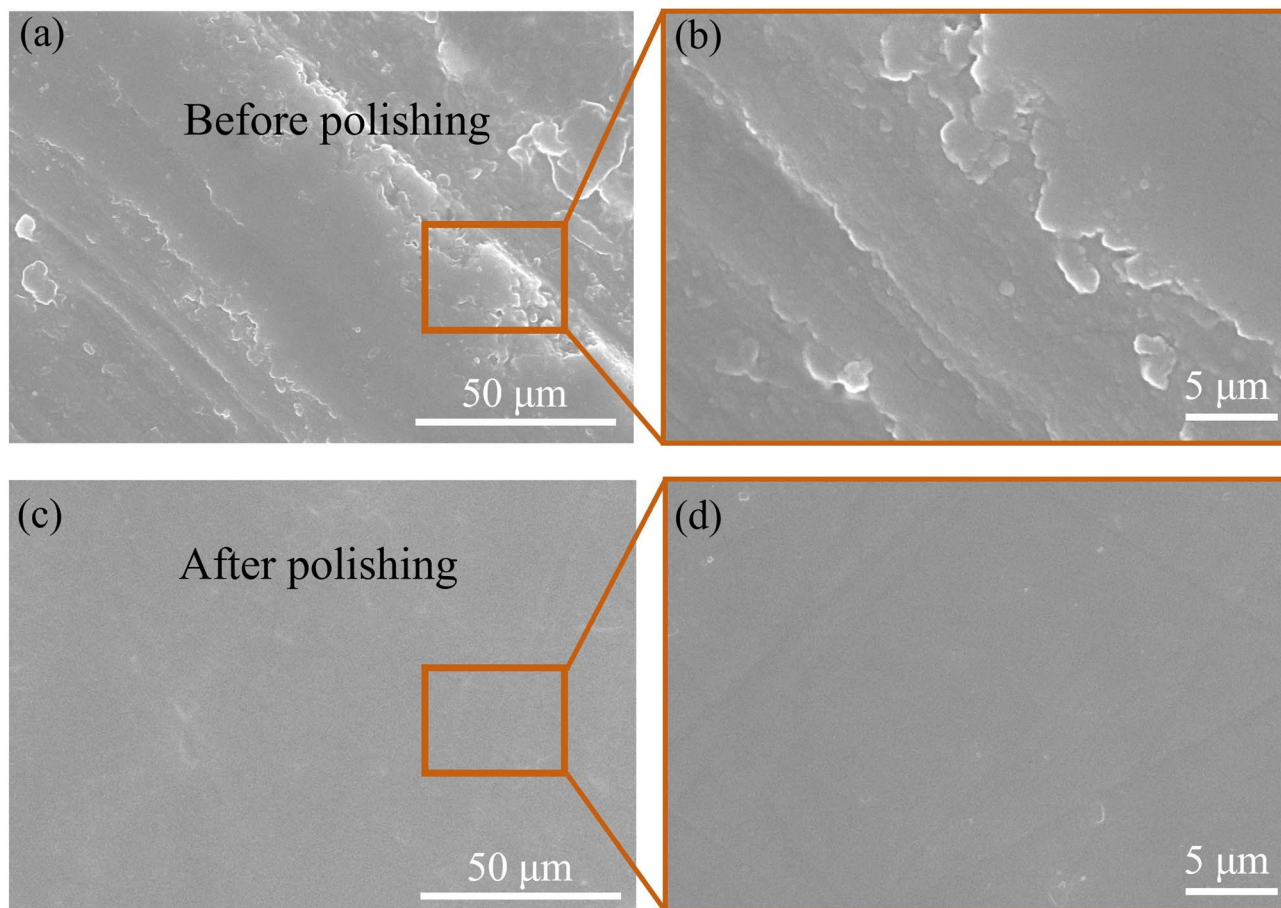


Fig. 12. SEM images of surface topography on the dental veneer before and after polishing.

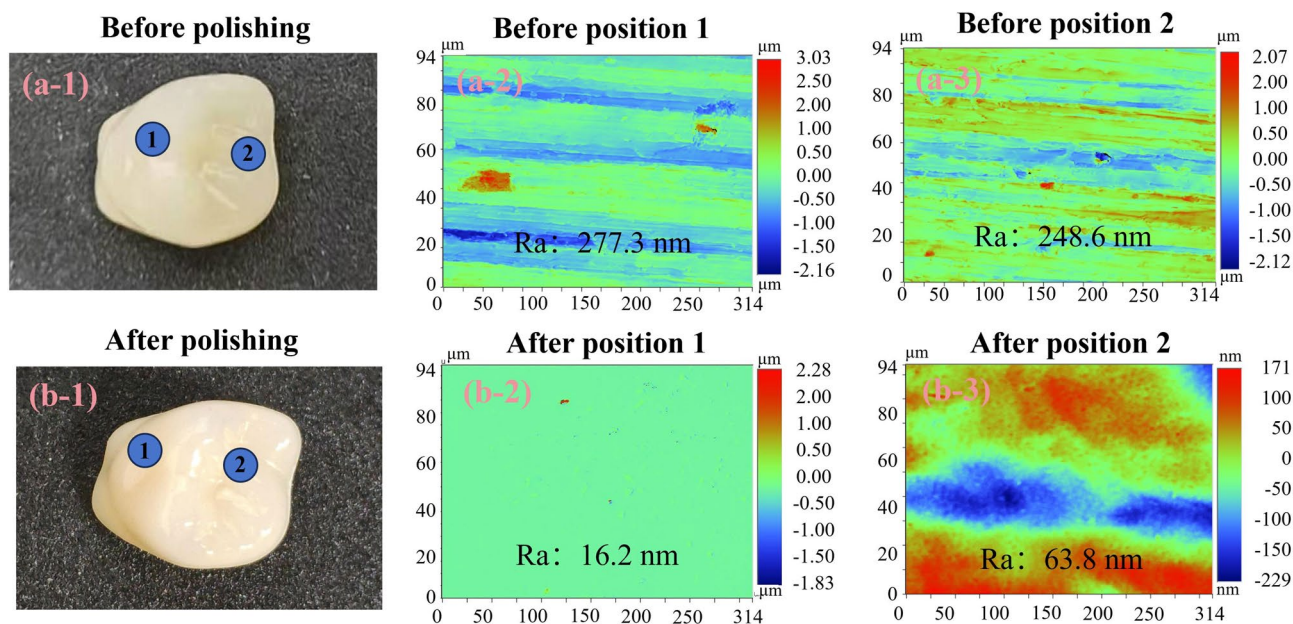


Fig. 13. Polishing performance on the dental crown using STF.

achieving nanoscale surface finish; Second, the average flexural strength after polishing reaches 816.2 MPa, with no statistically significant degradation in mechanical strength, indicating that the process relies exclusively on mechanical abrasion without inducing chemical damage. Currently, the feasibility of this method has been validated primarily at the laboratory scale through in vitro experiments. Nevertheless, further studies are required to evaluate post-polishing wear resistance and long-term biocompatibility in clinical settings.

In summary, the proposed STF-based polishing technique offers a highly efficient, cost-effective, and environmentally sustainable solution for ultra-precision finishing of dental ceramics, though clinical validation remains necessary to confirm its practical applicability.

Data availability

All data generated or analysed during this study are included in this published article and its supplementary information files.

Received: 23 December 2025; Accepted: 31 January 2026

Published online: 03 February 2026

References

- Shishido, S. et al. Residual stress associated with crystalline phase transformation of 3–6 mol% yttria-stabilized zirconia ceramics induced by mechanical surface treatments. *J. Mech. Behav. Biomed. Mater.* **146**, 106067 (2023).
- Wertz, M. et al. Phase transformations in yttria-partly stabilized zirconia induced by dental Polishing regimes. *J. Mater. Sci.* **59**, 6479–6496. (2024).
- Chen, L. et al. Comparison of bacterial adhesion and biofilm formation on zirconia fabricated by two different approaches: an in vitro and in vivo study. *Adv. Appl. Ceram.* **119**, 323–331 (2020).
- Koudriavtsev, T. V. & Villalobos, J. S. Crystallographic and topographic analysis of Ultra-Translucent zirconia after various surface Treatments, Odovtos. *Int. J. Dent. S.* **26**, 101–112 (2024).
- Aurelio, I. L., Marchionatti, A. M. E., Montagner, A. F., May, L. G. & Soares, F. Z. M. Does air particle abrasion affect the flexural strength and phase transformation of Y-TZP? A systematic review and meta-analysis. *Dent. Mater.* **32**, 827–845 (2016).
- Zhang, F., Reveron, H., Spies, B. C., Van Meerbeek, B. & Chevalier, J. Trade-off between fracture resistance and translucency of zirconia and lithium-disilicate glass ceramics for monolithic restorations. *Acta Biomater.* **91**, 24–34 (2019).
- Hashemikamangar, S. S., Nahavandi, A. M., Daryadar, M., Valizadeh, S. & Özcan, M. Effect of glazing and Polishing on opalescence and fluorescence of dental ceramics. *Clin. Exp. Dent. Res.* **8**, 1645–1654 (2022).
- Makkeyah, F., Moustafa, D. M., Bakr, M. M. & Al Ankily, M. Effect of two different intraoral Polishing systems on surface Roughness, color Stability, and bacterial accumulation of Zirconia-Reinforced lithium silicate ceramic. *Eur. J. Dent.* **18**, 1069–1075 (2024).
- Atash, R. et al. Evaluation of the effectiveness of four composite Polishing systems: an in vitro study. *Int. J. Periodont Rest.* **14**, 16–22 (2024).
- Zhang, Y., Vardhaman, S., Rodrigues, C. S. & Lawn, B. R. A critical review of dental lithia-based glass-ceramics. *J. Dent. Res.* **102**, 245–253 (2023).
- Edelhoff, D., Erdelt, K. J., Stawarczyk, B. & Liebermann, A. Pressable lithium disilicate ceramic versus CAD/CAM resin composite restorations in patients with moderate to severe tooth wear: clinical observations up to 13 years. *J. Esthet Restor. Dent.* **35**, 116–128 (2023).
- Pyo, S. W., Kim, D. J., Han, J. S. & Yeo, I. S. L. Ceramic materials and technologies applied to digital works in implant-supported restorative dentistry. *Materials* **13**, 1964 (2020).
- Ji, B., Alrayes, A. A., Zhao, J., Feng, Y. & Shen, Z. Grinding and Polishing efficiency of a novel self-glazed zirconia versus the conventional dry-pressed and sintered zirconia ceramics. *Adv. Appl. Ceram.* **118**, 46–55 (2019).
- Yuki, I. et al. Dry precision Polishing of dental composite resin: development of sodium alginate bonded mounted wheel. *J. Prosthodont. Res.* **62** (6), 318–323 (2016).
- Mokhtar, A. G., Hussein, G. & Wahsh, M. Effect of different surface treatments on bond strength of resin cement with lithium silicate Ceramics, Al-Azhar. *J. Dent. Sci.* **27**, 47–57 (2024).
- Cunha, W. et al. Surface modification of zirconia dental implants by laser texturing. *Lasers Med. Sci.* **37**, 1–17 (2022).
- Loh, Y. M. et al. A novel magnetic field assisted automatic batch Polishing method for dental ceramic crowns. *Ceram. Int.* **49**, 26540–26547 (2023).
- Wu, Z. et al. Research on Polishing aluminum alloy optical elements with a new solid flexible Bonnet tool. *J. Manuf. Process.* **103**, 168–180 (2023).
- Cao, Z. C., Wang, M., Yan, S., Zhao, C. & Liu, H. Surface integrity and material removal mechanism in fluid jet Polishing of optical glass. *J. Mater. Process. Technol.* **311**, 117798 (2023).
- Amir, M. et al. Development of magnetic nanoparticle based nanoabrasives for magnetorheological finishing process and all their variants. *Ceram. Int.* **49**, 6254–6261 (2023).
- Li, M. et al. Adaptive shearing-gradient thickening Polishing (AS-GTP) and subsurface damage Inhibition. *Int. J. Mach. Tools Manuf.* **160**, 103651 (2021).
- Li, M., Lyu, B., Yuan, J., Dong, C. & Dai, W. Shear-thickening Polishing method. *Int. J. Mach. Tools Manuf.* **94**, 88–99 (2015).
- Gürgen, S. & Sert, A. Polishing operation of a steel bar in a shear thickening fluid medium. *Compos. B Eng.* **175**, 107127 (2019).
- Span, J., Koshy, P., Klocke, F., Müller, S. & Coelho, R. Dynamic jamming in dense suspensions: surface finishing and edge honing applications. *CIRP Ann.* **66**, 321–324 (2017).
- Shao, Q. et al. Shear thickening Polishing of the concave surface of high-temperature nickel-based alloy turbine blade. *J. Mater. Res. Technol.* **11**, 72–84 (2021).
- Nguyen, D. N., Lyu, H. A. & Duong, C. T. Simulation study on Polishing of gear surfaces in non-Newtonian fluid. *Sci. Technol. Developm J. Eng. Technol.* **3**, 443–451 (2020).
- Ly, D. et al. Analysis of abrasives on cutting edge Preparation by drag finishing. *Int. J. Adv. Manuf. Tech.* **119.5**, 3583–3594 (2022).
- Azami, A. et al. A new theoretical model for surface roughness prediction in rotational abrasive finishing process. *Wear* **524**, 204772 (2023).

Acknowledgements

The authors would sincerely thank the reviewers for their very professional suggestions on this work.

Author contributions

Conceptualization, X.D.; investigation and writing, X.D., L.Z. and J.W.; software, X.D. and L.Z.; writing—review and editing, Z.Z., L.Z. and J.W.; visualization, Z.Z. and Z.Z.; funding acquisition, X.D., and Z.Z. All authors have read and agreed to the published version of the manuscript.

Funding

The research work was funded by the Natural Science Foundation of Zhejiang (No. JXSQY26E050002), and the Jiaxing's Key Research and Development Plan Projects (No. 2025AC013).

Declarations

Competing interests

The authors declare no competing interests.

Additional information

Supplementary Information The online version contains supplementary material available at <https://doi.org/10.1038/s41598-026-38788-x>.

Correspondence and requests for materials should be addressed to X.D.

Reprints and permissions information is available at www.nature.com/reprints.

Publisher's note Springer Nature remains neutral with regard to jurisdictional claims in published maps and institutional affiliations.

Open Access This article is licensed under a Creative Commons Attribution-NonCommercial-NoDerivatives 4.0 International License, which permits any non-commercial use, sharing, distribution and reproduction in any medium or format, as long as you give appropriate credit to the original author(s) and the source, provide a link to the Creative Commons licence, and indicate if you modified the licensed material. You do not have permission under this licence to share adapted material derived from this article or parts of it. The images or other third party material in this article are included in the article's Creative Commons licence, unless indicated otherwise in a credit line to the material. If material is not included in the article's Creative Commons licence and your intended use is not permitted by statutory regulation or exceeds the permitted use, you will need to obtain permission directly from the copyright holder. To view a copy of this licence, visit <http://creativecommons.org/licenses/by-nc-nd/4.0/>.

© The Author(s) 2026